

Article

A New Ex Vivo Model to Evaluate the Hair Protective Effect of a Biomimetic Exopolysaccharide against Water Pollution

Claire Tubia ¹, Alfonso Fernández-Botello ² , Jan Dupont ³, Eni Gómez ², Jérôme Desroches ³, Joan Attia ^{1,*}  and Estelle Loing ¹

¹ R&D, Lucas Meyer Cosmetics, 31036 Toulouse, France; claire.tubia@lucasmeyercosmetics.com (C.T.); estelle.loing@iff.com (E.L.)

² R&D, Centro de Tecnología Capilar, 08029 Barcelona, Spain; alfonsofernandez@ctc-cabello.com (A.F.-B.); enigomez@ctc-cabello.com (E.G.)

³ R&D, KAMAX Innovative System, 87069 Limoges, France; j.dupont@kamax-innovative.com (J.D.); j.desroches@kamax-innovative.com (J.D.)

* Correspondence: joan.attia@lucasmeyercosmetics.com

Received: 27 August 2020; Accepted: 29 September 2020; Published: 4 October 2020



Abstract: As an external appendage, hair is exposed to multiple stresses of different origins such as particles and gases in air, or heavy metals and chemicals in water. So far, little research has addressed the impact of water pollution on hair. The present study describes a new ex vivo model that allowed us to document the adverse effects of water pollutants on the structure of hair proteins, as well as the protective potential of active cosmetic ingredients derived from a biomimetic exopolysaccharide (EPS). The impact of water pollution was evaluated on hair from a Caucasian donor repeatedly immersed in heavy metal-containing water. Heavy metal retention in and on hair was then quantified using Inductively Coupled Plasma Spectrometry (ICP/MS). The adverse effects of heavy metals on the internal structure of hair and its prevention by the EPS were assessed through measurement of keratin birefringence. Notably, the method allows the monitoring of the organization of keratin fibers and therefore the initial change on it in order to modulate the global damage in the hair. Results revealed an increasing amount of lead, cadmium and copper, following multiple exposures to polluted water. In parallel, the structure of keratin was also altered with exposures. However, heavy metal-induced keratin fiber damage could be prevented in the presence of the tested EPS, avoiding more drastic hair problems, such as lack of shine, or decrease in strength, due to damage accumulation.

Keywords: water pollution; hair treatment; exopolysaccharide; keratin birefringence; polarimetric image analysis

1. Introduction

The condition of a human internal hair fiber, crucial for the physical properties of the hair, is traditionally determined by measuring its mechanical stress–strain characteristics [1] or by evaluating the state of its surface, using scanning electron microscopy or atomic force microscopy technologies [2,3].

Hair fiber is composed of three layers, the cuticle, the cortex and the medulla. The cortex is the main layer of hair fiber and responsible for mechanical property with macrofibrils or intermediate filaments, composed of keratin [4]. Taking into account that more than 85% of the weight of hair comes from keratin [5], it seems reasonable to assume that any alterations in the condition of hair, as documented with the techniques mentioned above, would be due to changes in its major component, keratin [6]. So, to the best of our knowledge, it is crucial to detect the first change in the protein in order to avoid more dramatic change in the hair properties. Keratins belongs to a family of fibrous

structural proteins known as scleroproteins that usually display a hexagonal shape [7]. Due to its molecular structure, the protein manifests birefringence when placed in a field of polarized light [8]. As a decrease in birefringence is deeply related to the loss of protein structure [9,10], measurement of this property allows the detection of any change that may affect the hair at the molecular level.

Since hair is constantly in contact with the environment, one of the most important aggressions it suffers comes from air and water pollution. It is well documented that polluted air impacts hair surface properties [11], while sea water or even hard water may cause fiber stiffening [12]. Moreover, various pollutants, including heavy metals with a high aquatic solubility, can interact with hair and certainly damage hair fibers. Taking into account that, by 2050, about one third of the world population will not have access to a reliable source of water [13] and that clean water is not only a basic need for human beings but also has a great influence on all aspects of human life [14,15], it is clear that research on products and ingredients offering protection against water pollution has become of primary importance [16,17].

Water contamination has many sources. Industrialization and urbanization are two of the main culprits for the increasing levels of heavy metals seen in water [18]. When people use this polluted water for their daily activities, pollutants can be assimilated by their body through different routes, including inhalation and ingestion, as well as skin and hair absorption. Indeed, traces of heavy metals have been demonstrated to be induced by lifestyle (smoking) [19]. Considering that hair has been selected by the World Health Organization (WHO) and Environment Protection Agency for the assessment of toxic metal influence on human organism [20], and that keratin-reactive sites can interact with metal ions [21–23], this paper aims at addressing the effects of heavy metal-contaminated water on the molecular structure of hair, especially on keratin, to avoid potential major damage in the hair such as lack of shine, vitality, etc. For this purpose, a polluted water model was developed and validated, based on data obtained from a toxicological evaluation of the river Yamuna, in the Indian city of Agra [24]. Birefringence signal due to keratin structure and organization was studied in Caucasian hair strands provided by a unique donor. Using this model, the impact of water pollution on internal hair structure and the protective potential of a biomimetic exopolysaccharide (EPS) were evaluated *ex vivo*. EPS are high molecular weight carbohydrates with a biofilm property secreted by microorganisms into their environment. EPS vary greatly in their composition which impacts their chemical and physical properties. Many reports have described marine bacterial EPS to have high metal binding thanks to their higher uronic acid content, which enhances anionicity [25].

2. Materials and Methods

2.1. Exopolysaccharide

The EPS used for the present study was obtained through fermentation of a marine strain of *Alteromonas macleodi* isolated from the French Polynesian kopara. This EPS is a highly ramified polysaccharide composed of neutral sugars as rhamnose, fucose, mannose, glucose and galactoses (57%), uronic acids as glucuronic and galacturonic acid (25%), and sulfates (8%). It is also rich in essential minerals such as potassium, sodium, magnesium and calcium.

2.1.1. Potential Zeta Measurement

The EPS potential zeta measurement has been analyzed with the Zetasizer Nano ZS (Malvern). Analysis was realized under 25 °C, with a count rate of 350.6 kcps, and a zeta runs of 12. Measurement was performed in triplicate.

2.1.2. Chelation Analysis

Heavy metals removing efficiency is analyzed *in vitro*. A solution containing 10 g/L of EPS and 100 ppb of arsenic, cadmium, lead and mercury was made. After 3 h of incubation at 25 °C, the sample was centrifuged and filtered. The supernatant solution, the dried raw material (EPS exposed to heavy

metals) and an untreated raw material (EPS not exposed) were analyzed by Inductively Coupled Plasma Spectrometry (ICP/MS) for heavy metal content.

2.2. Polluted Water Model

To mimic the effect of water pollution on hair, a model of heavy metal-polluted water was developed, based on data obtained from a toxicological evaluation of the river Yamuna, in the Indian city of Agra [24]. As pollution of this river mainly results from human activities (agriculture, industrialization, urbanization), the model is therefore considered as representative of global water pollution.

Polluted water was prepared with dilution of concentrated commercial standards of the elements of interests (Pb, Zn, Cu, Cd, Cr, Ag, Hg and Fe), and addition and dissolution of the proper amount of pure solid sodium carbonate (Na_2CO_3) in distilled water (see Table 1). Once the dissolution is ready, the theoretical concentrations are checked by ICP/MS analysis of the elements present (Pb, Zn, Cu, Cd, Cr, Ag, Hg, Fe and Na). When the concentration was under detection limits of the machine, “<0.01” was indicated.

Table 1. Heavy metal and mineral concentrations in the polluted water model.

Heavy Metal	Lead (Pb)	Zinc (Zn)	Copper (Cu)	Cadmium (Cd)	Chrome (Cr)	Mercury (Hg)	Silver (Ag)	Calcium Carbonate	Iron (Fe)
mg/L	0.428	3.420	7.085	0.865	0.662	<0.01	0.01	180	<0.03

2.3. Analysis of Heavy Metal Levels in Hair, Following Exposure to Polluted Water

Strands of healthy hair from a single Caucasian donor were used. Hair strands were prewashed, rinsed in either distilled water (control) or polluted water and then left to dry. Following 10 immersions into polluted water, representative of 1 or 2 weeks of daily exposure, 50 mg of hair samples was mineralized in nitric acid (sigma) for metal retention quantification using Inductively Coupled Plasma Spectrometry (ICP/MS). Analyses were completed on a XSeries II (Thermo Electron) equipped with a Meinhard nebulizer. The analysis was done with a plasma power at 1450 W; a nebulizer gas flow of 1.016 L/min, the coolant gas flow of 1.016 L/min, 50 sweeps and 10 ms per isotope of dwell time. Retention of exogenous lead, cadmium and copper was documented.

2.4. Heavy Metal Impacts on Hair Structure, with and without EPS

2.4.1. Exposure of Hair to Polluted Water

Strands of healthy hair from the same single Caucasian donor were used to document the impact of polluted water exposure on hair structure. Hair strands were prewashed, then three groups of 41 hair fibers were selected. One group was first immersed for 2 min in a solution containing the EPS (0.1 g/L), massaged for 1 min, then exposed to polluted water for 2 min. The second group was only exposed to polluted water for 2 min. The third group was immersed for 2 min in distilled water but received no further treatment and served as control. All hair strands were next massaged for 30 s. According to the preliminary experiment, we decided to repeat this protocol 30 times, which is necessary to detect the significant impact of polluted water.

For hair structure analysis, for each of the 41 hair fibers, middle sections were cut into 2-cm lengths and mounted on different microscope slides, in Euparal mounting media ($n = 1535$). For each hair sample, keratin birefringence was measured at 3 distinct regions with a polarimetric scanner (K-PROBE[®] polarimetric scanner) and a mean keratin birefringence value was calculated.

2.4.2. Polarization Study of Hair Fibers

Theoretical Background on the Birefringence

Birefringent materials have the particularity to have two different refractive indexes, n_o (along the ordinary axis) and n_e (along the extraordinary axis), the birefringence being the dimensionless quantity $\Delta n = n_e - n_o$. When light passes through a birefringent sample, a phase difference θ (rad.) called retardance is produced between orthogonal projections of the light electric field [26], which is proportional to the birefringence Δn and birefringent thickness e crossed by the light upon reflection.

Retardance θ and birefringence Δn are linked with the equation:

$$\theta = (2\pi e \Delta n)/\lambda \quad (1)$$

with λ the wavelength.

We should emphasize that the “thickness” of hair at a given pixel impacts the retardance value (which is measured) but not the keratin birefringence (that we want to determine). In order to determine the birefringence value, we use a parametrized ovoid hair section model: its birefringence, diameter and shape are determined by a non-linear least square regression of the retardance signal. Thus, a potential hair asymmetry can be handled by the model.

Birefringence is an intrinsic parameter of the sample, depending on its material and structure. Retardance, however, also depends on the sample thickness.

The technique used in this study is based on the emission of a laser light on the sample; its state of polarization can take any value on the Poincaré sphere. The light reflected by a mirror under the sample is collected and the intensities polarized along two orthogonal states of polarization are measured: I_{\parallel} and I . The K_{max} parameter is then computed

$$K_{max} = \max\left\{\frac{I_{\parallel}}{I_{\parallel} + I}\right\} \quad (2)$$

The K_{max} value is linked to the sample retardance with [27]:

$$K_{max} = \sin^2(\theta/2) = \sin^2(\pi e \Delta n/\lambda) \quad (3)$$

The instrument gives a measure of the K_{max} value for each pixel of the field of view. Thus, it gives a value of the retardance applied to the light detected by each pixel. Contrarily to crossed polarizers microscopy [28], the retardance value measured by this technique is independent of rotation of the sample optic axis in the image plane, which allows quantitative characterization based on the sample retardance [29].

Theoretical Background on Hair Birefringence Measurement

In hair samples, the sample thickness e is unknown, and is spatially variant in the field of view. As it can be seen in Equation (3), the birefringence Δn cannot be distinguished from the thickness e using a K_{max} measurement, if these two parameters are unknown. Thus, in order to estimate the birefringence Δn , we must make an assumption about the sample thickness. For that purpose, we use a hair thickness model, based on an ovoid approximation of the hair section.

Let (x, y) be a plane perpendicular to the hair growth direction (z) with its origin on the hair center, and y be the direction of propagation of light. At a given position z along the hair, let R be the hair radius and r the medulla radius, $r < R$, which describes an area at the center of the hair where the material has a low birefringence. We also introduce an “ovoid” factor k , describing a potential asymmetry of the hair section. Then the birefringent thickness $e(x)$ crossed by the light upon reflection is:

$$e(x) = 4R\sqrt{[(1 - x^2/R^2) * R^2/(1 + kx)]} - 4R\sqrt{(r^2 - x^2)} \quad (4)$$

Hair Fiber Birefringence Measurement

Hair fiber birefringence was measured with the K-PROBE[®] POLARIMETRIC SCANNER using the XPolar[®] technology, from Kamax Innovative System. The measurement is based on a contactless technique and the signal does not require any staining, which avoids any sample degradation. The wavelength of the source is 780 nm, the magnification is 400×, the image size is 800 × 600 pixels, each pixel covers an object area of about 0.25 μm².

An example of raw data measured by XPolar[®] is represented in Figure 1a, giving the Kmax values measured. The periodicity of the Kmax signal can be understood by looking at Equation (3), where one can notice the sin²(x) function, which has a kπ periodicity (k integer). The physical interpretation of this effect is that the retardance between orthogonal projections of the light electric field is evolving periodically between its minimum (for πeΔn/λ = kπ) and its maximum (for πeΔn/λ = kπ/2) depending on the material thickness e (and birefringence Δn) crossed by the light at the considered pixel.

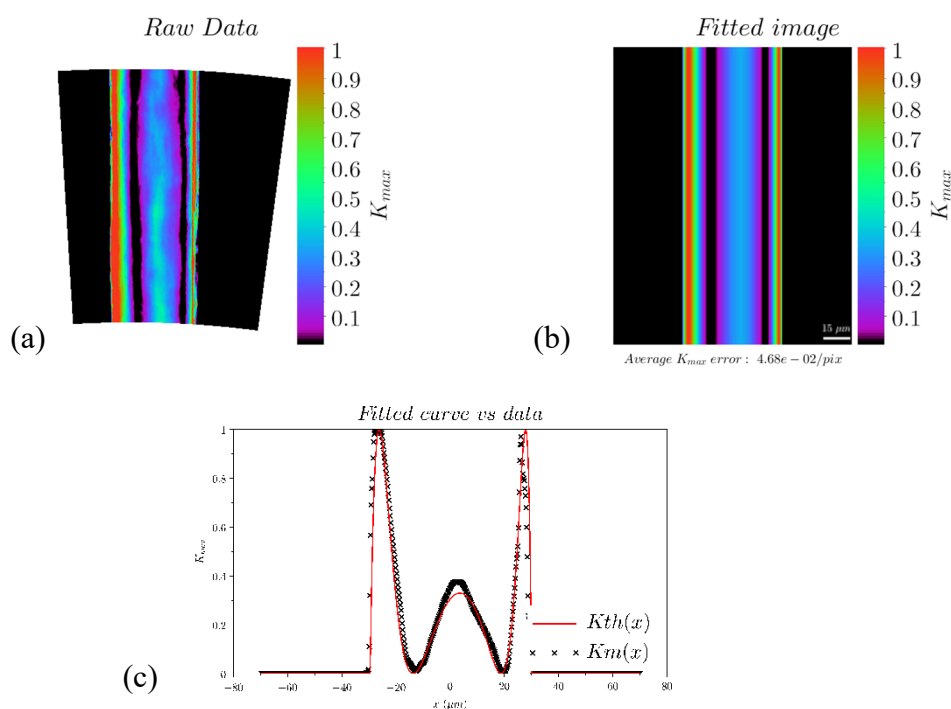


Figure 1. Example of Xpolar measurement and data analysis. (a) Kmax values experimentally measured. (b) Representation of the fitted image, by replication of the fitted curve $K_{th}(x)$ along the y direction. (c) Fitted theoretical curve (red) versus the averaged transverse Kmax variations (black), computed from the raw data.

In order to obtain the estimation of the hair birefringence, we compute the averaged transverse variations of the measured Kmax parameter on 500 lines of the Kmax image (called in the following $K_m(x)$), as plotted in Figure 1c, black). The $K_m(x)$ curve will be the input data used for the estimation of the global hair birefringence. By substitution of e in Equation (3) with its expression defined in Equation (4), one can notice that we have a theoretical expression of the Kmax parameter, in the form of four input parameters (hair radius R, medulla radius r, ovoid index k and keratin birefringence Δn), in Equation (5).

$$K_{max} = \sin^2(\theta/2) = \sin^2(\pi\Delta n 4R \{ \sqrt{[(1 - x^2/R^2) * R^2/(1 + kx)]} - 4R \{ \sqrt{(r^2 - x^2)} \} / \lambda) \quad (5)$$

The theoretical Kmax variations will be designated by $K_{th}(x,p)$, with p a vector containing the unknown parameters (R, r, k and Δn) (an example is plotted in Figure 1c, red curve). Estimation is performed by iterative assumptions of the four values of the parameters of the model $K_{th}(x,p)$,

in order to decrease the difference (least mean square difference) between the model $K_{th}(x,p)$ and the experimental data $K_m(x)$. When the difference is minimized, the modeled K_{max} values are the closest to the experimental K_{max} values and thus we have an estimation of the four parameters, including the birefringence Δn of the considered hair. An example of fitted $K_{th}(x,p)$ is represented in Figure 1c, red curve). Besides, by replication of $K_{th}(x,p)$ in the z direction, we construct a simulated image (Figure 1b) which can be compared with the raw K_{max} image (Figure 1a).

2.5. Statistical Analysis

To overcome effects of potential uncontrolled variables, we randomly build 3 sets of hairs coming from the same hair strand, which will experience the 3 different conditions. To search for differences between populations that may be influenced by 1 or more uncontrolled variables, the obtained data and percentage variations between two conditions were submitted to a one-sided student t-test for independent samples with unequal variances. The statistical significance value was considered at $p < 0.05$.

3. Results and Discussion

3.1. Heavy Metals Retention in Hair

Following 10 cycles of exposure to water, loaded or not with heavy metals, metal retention on the surface and inside hair fibers was quantified using Inductively Coupled Plasma Spectrometry (ICP/MS). Exposure to polluted water significantly increased hair concentrations of copper, cadmium and lead by 120%, 846% and 214% respectively, compared to control (Figure 2). Such significant increases validate our polluted water model to study the impact of water pollution on the structure of hair. The presence of zinc and calcium was also recorded, however, substantial quantities of these minerals are naturally found in hair fibers.

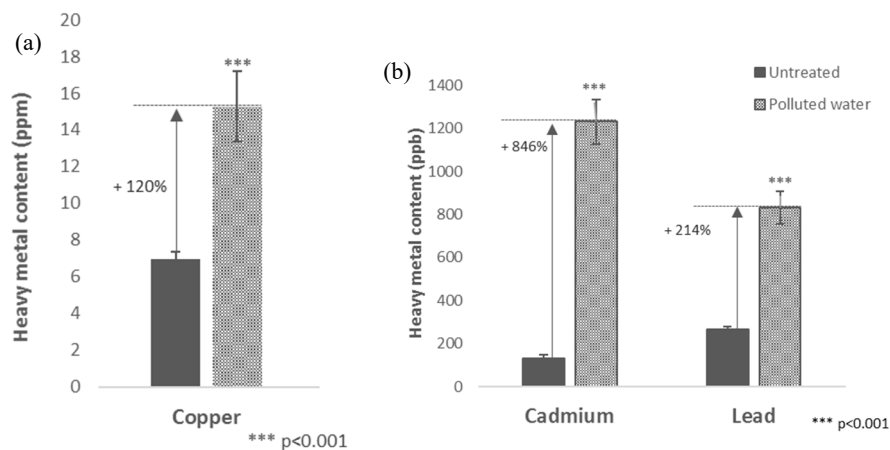


Figure 2. Repetitive exposure to polluted water increases heavy metal content on and in hair fibers. (***) $p < 0.001$. (a) Copper content is expressed in parts per million. (b) Cadmium and lead content are expressed in parts per billion.

Hair is essentially made of keratin, a fibrous structural protein of major importance for the mechanical properties and appearance of hair. Within hair, keratin fibers are held together through various types of bonds (hydrogen, salt and disulfide bonds). Besides their structural role, these bonds also provide soft spots through which the environment can affect the hair. For instance, human hair has a strongly negative surface charge mainly due to the anionic molecules in their composition, such as glutamic acid and aspartic acid. Taking into account that glutamic acid and aspartic acid make up for 25.9% of the total amino acid composition of keratin [30], and that keratin is the main protein responsible of hair physical properties [6], it is clear that any interaction with this components will

have an impact in the hair properties. As water pollutants are essentially mono- or di-valent cations, they have a strong attraction for the negative charge of hair, and thanks to their size can penetrate inside the fiber to interact with the internal bonds responsible for the hair structure.

Here we show that hair repeatedly exposed to polluted water significantly retains cationic heavy metals such as copper, cadmium and lead. The retention can be explained by interactions forming ionic bonds between hair and pollutants. Once heavy metals have penetrated within the hair, they bind to keratin with the potential to affect its structure and therefore their functions.

3.2. Impact of Polluted Water and Protective Potential of the Biomimetic EPS

The exopolysaccharide used in this study was chosen for its chemical property. Indeed, it presents high molecular weight which confers him filmogenic property. Furthermore, with its composition, rich in uronic acid groups and its negative potential zeta (-16.4 mV), the product has proven its efficiency to chelate heavy metals (Table 2). Table 2 shows the decrease in heavy metals in an aqueous solution after contact with the EPS.

Table 2. Heavy metal and mineral concentrations in the polluted water model.

Metal	Exopolysaccharide (EPS) Material without Any Exposure	EPS Material after Exposure to Heavy Metals	Liquid Pre-Incubation	Liquid Post Incubation
Arsenic	0.033 ppm	44.0 ppm	100 ppb	<10 ppb
Cadmium	0.082 ppm	45.9 ppm	100 ppb	<1.0 ppb
Lead	0.150 ppm	53.1 ppm	100 ppb	<10 ppb
Mercury	0.015 ppm	342 ppm	100 ppb	<5.0 ppb

The impact of heavy metal retention on the structure of hair and the protective potential of EPS were documented at the molecular level through the measurement of changes in keratin birefringence, using K-Probe[®] polarimetric scanner technology associated with the XPolar[®] imagery system. The determination at the molecular level allow us to determine the initial change in the keratin structure.

Figure 3 displays the representative experimental images resulting from birefringence analysis, representative of the average retardance of their respective hair set (bottom panels) and the corresponding fitted theoretical composition retardance of hairs obtained with the theoretical model (top panels) in various conditions. A typical result for the control group is shown in the left panels, for the polluted water-challenged group in the middle panels, and for the EPS-pre-treated group in the right panels. Clearly, immersion in polluted water changes the hair birefringence response compared to control, revealing that the internal structure of hair has been modified by the challenge. However, pre-treating the hair with the biomimetic EPS (0.1 g/L) negates the effect of water pollution and restores hair response to light seen in control, attesting of the protective effect of the EPS on global keratin fiber structure.

Despite the major visual impact of these images, they are only tools through which hair birefringence values can be obtained, in order to measure the impact of polluted water on proteins structure. The average birefringence values calculated from these images for each hair fiber is shown in Table 3 (average of at least three points measurement of measure from the same hair fiber) and reviewed in Figure 4 with standard deviation.

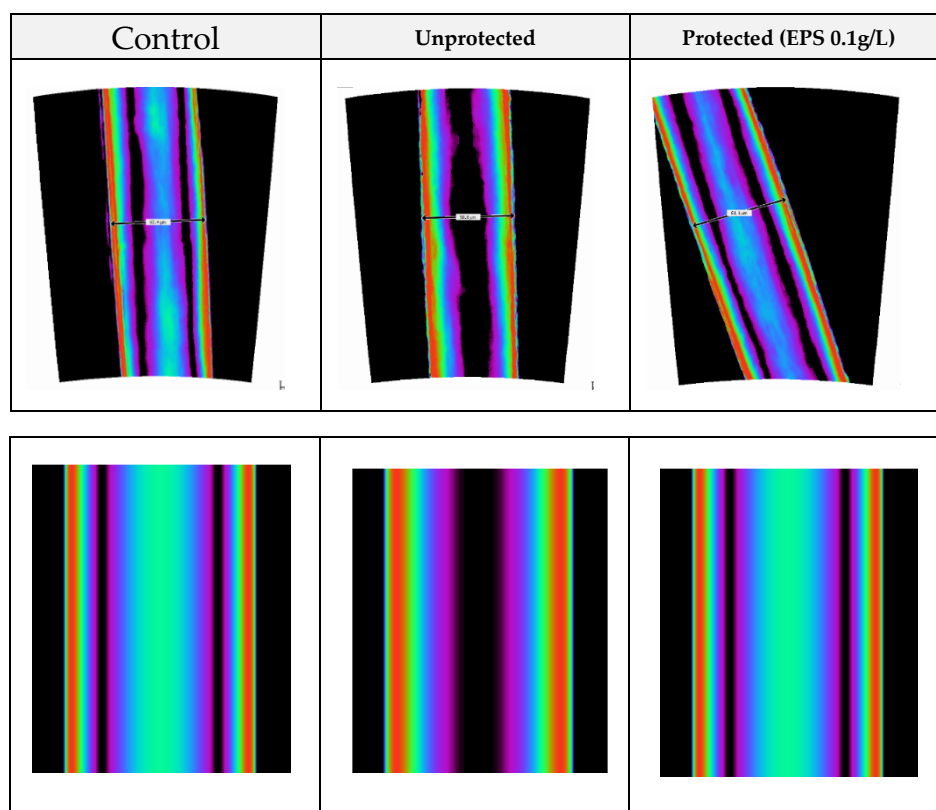


Figure 3. Representative photography of hair section analyzed with K-PROBE[®] polarimetric scanner. Kmax experimental images (top panels) and the corresponding fitted image (bottom panels) obtained for a hair diameter of approximately 60 μm , following immersion in heavy metal-containing water without (middle panels) and with EPS pre-treatment (right panels), compared to control (left panels).

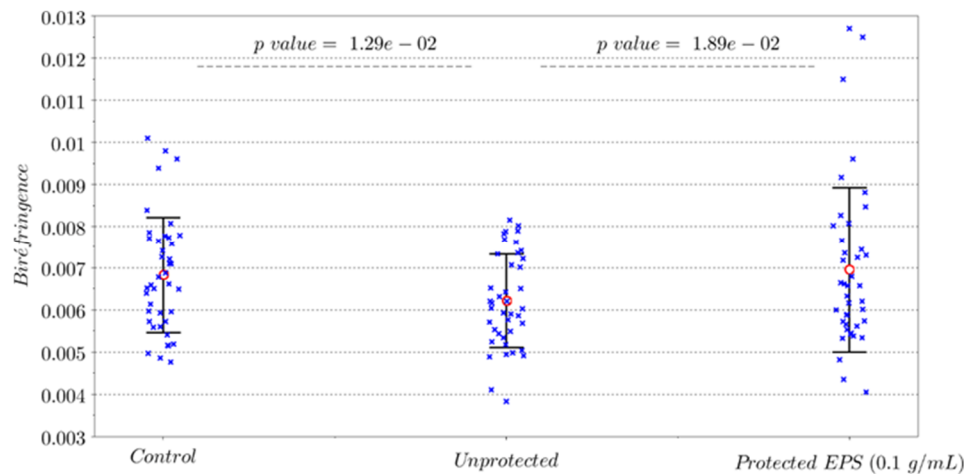
Table 3. Average birefringence values.

	Control Birefringence	Unprotected Birefringence	Protected Birefringence
Hair 1	4.77×10^{-3}	5.18×10^{-3}	7.25×10^{-3}
Hair 2	7.65×10^{-3}	7.62×10^{-3}	6.57×10^{-3}
Hair 3	5.93×10^{-3}	6.17×10^{-3}	5.72×10^{-3}
Hair 4	5.41×10^{-3}	8.15×10^{-3}	6.01×10^{-3}
Hair 5	7.72×10^{-3}	7.33×10^{-3}	5.45×10^{-3}
Hair 6	1.01×10^{-2}	5.93×10^{-3}	1.15×10^{-2}
Hair 7	6.87×10^{-3}	7.82×10^{-3}	6.62×10^{-3}
Hair 8	8.07×10^{-3}	6.52×10^{-3}	8.26×10^{-3}
Hair 9	7.26×10^{-3}	7.07×10^{-3}	9.17×10^{-3}
Hair 10	7.41×10^{-3}	5.34×10^{-3}	7.44×10^{-3}
Hair 11	4.97×10^{-3}	5.86×10^{-3}	6.16×10^{-3}
Hair 12	7.85×10^{-3}	4.89×10^{-3}	5.38×10^{-3}
Hair 13	6.52×10^{-3}	6.20×10^{-3}	4.06×10^{-3}

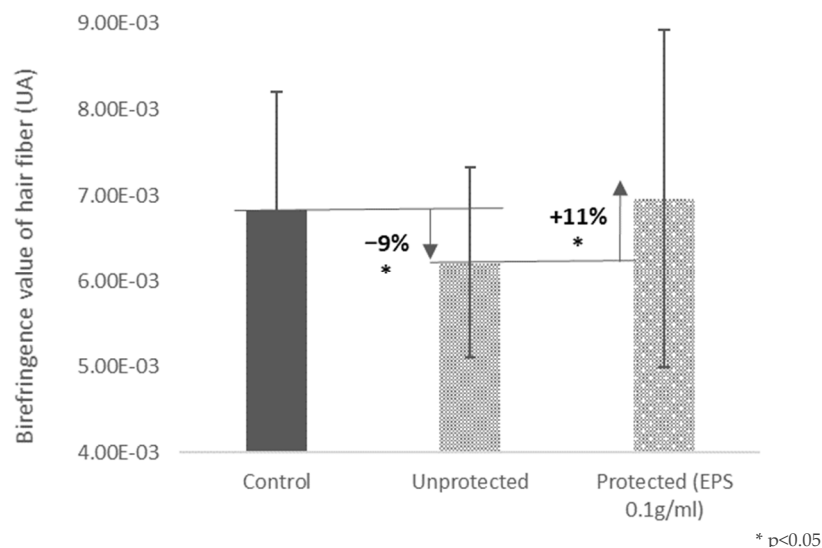
Table 3. Cont.

	Control Birefringence	Unprotected Birefringence	Protected Birefringence
Hair 14	9.39×10^{-3}	7.88×10^{-3}	7.30×10^{-3}
Hair 15	7.20×10^{-3}	5.69×10^{-3}	4.35×10^{-3}
Hair 16	6.59×10^{-3}	7.22×10^{-3}	7.36×10^{-3}
Hair 17	5.59×10^{-3}	5.25×10^{-3}	7.66×10^{-3}
Hair 18	5.60×10^{-3}	6.51×10^{-3}	8.47×10^{-3}
Hair 19	4.86×10^{-3}	5.49×10^{-3}	8.01×10^{-3}
Hair 20	9.80×10^{-3}	4.92×10^{-3}	5.33×10^{-3}
Hair 21	5.72×10^{-3}	4.11×10^{-3}	8.07×10^{-3}
Hair 22	5.97×10^{-3}	7.41×10^{-3}	6.33×10^{-3}
Hair 23	7.77×10^{-3}	6.02×10^{-3}	5.89×10^{-3}
Hair 24	7.71×10^{-3}	3.84×10^{-3}	6.00×10^{-3}
Hair 25	5.16×10^{-3}	6.32×10^{-3}	5.54×10^{-3}
Hair 26	6.40×10^{-3}	6.04×10^{-3}	6.57×10^{-3}
Hair 27	7.10×10^{-3}	5.91×10^{-3}	5.34×10^{-3}
Hair 28	6.62×10^{-3}	6.21×10^{-3}	4.82×10^{-3}
Hair 29	7.09×10^{-3}	5.54×10^{-3}	5.61×10^{-3}
Hair 30	6.49×10^{-3}	5.04×10^{-3}	5.42×10^{-3}
Hair 31	6.13×10^{-3}	5.44×10^{-3}	5.74×10^{-3}
Hair 32	5.96×10^{-3}	6.43×10^{-3}	5.87×10^{-3}
Hair 33	5.73×10^{-3}	4.95×10^{-3}	9.60×10^{-3}
Hair 34	5.19×10^{-3}	4.99×10^{-3}	6.79×10^{-3}
Hair 35	8.38×10^{-3}	7.35×10^{-3}	6.20×10^{-3}
Hair 36	5.15×10^{-3}	5.71×10^{-3}	7.18×10^{-3}
Hair 37	7.57×10^{-3}	5.76×10^{-3}	8.81×10^{-3}
Hair 38	6.51×10^{-3}	8.02×10^{-3}	6.65×10^{-3}
Hair 39	7.78×10^{-3}	7.02×10^{-3}	1.25×10^{-2}
Hair 40	9.61×10^{-3}	7.68×10^{-3}	1.27×10^{-2}
Hair 41	6.78×10^{-3}	7.89×10^{-3}	5.65×10^{-3}
Average birefringence by condition	6.84×10^{-3}	6.21×10^{-3}	6.96×10^{-3}

What does a change in birefringence really mean? In order to understand the meaning of our experiment, we can provide an example taking into account that birefringence is defined as the difference between the two refractive indices of an optically anisotropic material. Imagine that we have two elements with the same diameter and composition but with a very different density or structure. The difference of their two refractive indices will be quite distinct and therefore so would be the difference in their birefringence. On the other hand, if these two elements have the same density and structure, light will be refracted in the same way and thus the difference of their refractive indices and their birefringence would be quite identical. Now, if we were to submit one of the twin materials to an attack capable of affecting its density and structure, then the refractive indices difference and birefringence of the two would become divergent.



(a)



(b)

Figure 4. (a) Birefringence values, as measured on a total of 41 hairs for control, unprotected, and EPS-protected hair (0.1 g/mL). Blue cross: birefringence of one hair averaged from two measures. Red circle: average birefringence of 41 hairs. Black line: \pm one standard deviation of the birefringence of 41 hairs. The p values are computed using one sided Student's t -test for independent samples with unequal variances. (b) Mean birefringence value and standard deviation for each condition (* $p < 0.05$ versus control).

Since the structure of hair in the control group (with no heavy metal challenge) is considered intact, the birefringence values obtained for this group can thus be taken as the basal levels for all hair samples. Following 30 cycles of exposure to polluted water without protection, the mean birefringence values decreased by 9% compared to control, with a p -value < 0.05 , meaning that the impact of polluted water on hair fiber is statistically significant. However, with EPS (0.1 g/L) pre-treatment of hair fibers birefringence is not significantly different from the control but significantly different to placebo, by 11% (p -value < 0.05). The decrease in birefringence seen when hair fibers are attacked by water pollutants (compared to control) reflects a loss of structural integrity in keratin. If this damage is not stopped, it should have definite impact on the macromolecular properties of hair, for example dry, damaged, and less stretchy hair. Fortunately, pre-treating hair with the biomimetic EPS (0.1 g/L) restores birefringence values back to basal levels, avoiding initial damage of keratin structure. EPS effectively and fully protects hair keratin from water pollution-induced structural changes.

After confirming in our model, the attraction of heavy metal by hair fiber, we demonstrate the impact of heavy metals content in hair on keratin structure, the main protein of hair fiber. To further study heavy metals penetration and EPS effect, an analysis of heavy metals inside the hair fiber could give supplemented information, that we could not have with ICP/MS analysis. However, to the best of our knowledge, some inherent characteristics of the biomimetic EPS may play a role in hair protection. For one, the high molecular weight and the composition of the EPS would confer protective filmogenic properties that create a physical barrier on hair against pollutants. Furthermore, our chelating property of the EPS may help by blocking adhesion of heavy metals to hair. Both properties synergize to prevent heavy metals from damaging the structure of keratin and should help to maintain the physical properties of hair.

4. Conclusions

As pollution levels rise around the world, consumers are increasingly concerned about the negative effects it may have on their body and hair. Several scientific studies have already documented harmful effects of air pollution on skin and hair but little research has been done so far on the impact of water pollution on these structures.

This present study was aimed at developing a platform to assess the effects of water pollution on the internal structure of hair and test the protective potential of a cosmetic active ingredient derived from a biomimetic EPS. Results confirmed that water pollutants can indeed penetrate the hair, causing damages to keratin, its fibrous structural protein. Such detrimental effects of water pollution were prevented by protective filmogenic and chelating properties of EPS. Because keratin is the main structural protein of the hair, it is reasonable to suggest that this protection would also enable the preservation of the physical properties of the hair such as strength and elasticity against repetitive and daily detrimental exposure.

Author Contributions: Conceptualization, C.T. and J.A.; Methodology, C.T. and A.F.-B.; Investigation and Writing, C.T., A.F.-B. and J.D. (Jan Dupont); Supervision E.G., J.D. (Jérôme Dupont) and E.L. All authors read and approved the final manuscript.

Funding: This research received no external funding.

Acknowledgments: The authors wish to thank all the team of Synelvia laboratory for their valued help in the heavy metal analysis in hair.

Conflicts of Interest: The authors declare no conflict of interest.

References

1. Beyak, R.; Mlyer, C.F.; Kass, G.S. Elasticity and tensile properties of human hair. I. Single fiber test method. *Soc. Cosm. Chem.* **1969**, *20*, 615–626.
2. Kaliyadan, F.; Gosai, B.; Al Melhim, W.N.; Feroze, K.; Qureshi, H.A.; Ibrahim, S.; Kuruvilla, J. Scanning electron microscopy study of hair shaft damage secondary to cosmetic treatments of the hair. *Int. J. Trichol.* **2016**, *8*, 94. [[CrossRef](#)] [[PubMed](#)]
3. Bharat, B. Structural, nanomechanical, and nanotribological characterization of human hair and conditioner using atomic force microscopy and nanoindentation. In Proceedings of the Advances in Cosmetic Formulation Design, Columbus, OH, USA, 24 July 2018.
4. Robbins, C.R. *Chemical and Physical Behavior of Human Hair*, 3rd ed.; Springer: New York, NY, USA, 1994; 391p.
5. Gillespie, J.M.; Marshall, R.C. The Proteins of Normal and Aberrant Hair Keratins. In *Hair Research*; Orfanos, C.E., Montagna, W., Stüttgen, G., Eds.; Springer: Berlin/Heidelberg, Germany, 1981.
6. Velasco, M.V.R.; Dias, T.C.D.S.; De Freitas, A.Z.; Junior, N.D.V.; Pinto, C.A.S.D.O.; Kaneko, T.M.; Baby, A.R. Hair fiber characteristics and methods to evaluate hair physical and mechanical properties. *Braz. J. Pharm. Sci.* **2009**, *45*, 153–162. [[CrossRef](#)]
7. Ciferri, A. Translation of Molecular Order to the Macroscopic Level. *Chem. Rev.* **2015**, *116*, 1353–1374. [[CrossRef](#)]
8. Fraser, R.D.B. Birefringence and Elasticity in Keratin Fibres. *Nature* **1953**, *172*, 675–676. [[CrossRef](#)]

9. Feughelman, M. *Mechanical Properties and Structure of Alpha-Keratin Fibres: Wool, Human Hair, and Related Fibres*; UNSW Press: Sydney, Australia, 1997; pp. 41–42.
10. Mercer, E. Some experiments on the orientation and hardening of keratin in the hair follicle. *Biochim. Biophys. Acta (BBA) Bioenerg.* **1949**, *3*, 161–169. [[CrossRef](#)]
11. Galliano, A.; Ye, C.; Su, F.; Wang, C.; Wang, Y.; Liu, C.; Wagle, A.; Guerin, M.; Flament, F.; Steel, A. Particulate matter adheres to human hair exposed to severe aerial pollution: Consequences for certain hair surface properties. *Int. J. Cosmet. Sci.* **2017**, *39*, 610–616. [[CrossRef](#)]
12. Evans, A.O.; Marsh, J.M.; Wickett, R.R. The structural implications of water hardness metal uptake by human hair. *Int. J. Cosmet. Sci.* **2011**, *33*, 477–482. [[CrossRef](#)]
13. Unesco. World Water Development Report. Available online: <http://www.unesco.org/water/wwapconsulted> (accessed on 13 December 2019).
14. Ahmad, R. Studies on the chemistry control of some selected drinking and industrial waters. *Pakistan J. Sci. Ind. Res.* **2005**, *48*, 174–179.
15. Farid, S.; Kaleem-Baloch, M.; Amjad-Ahmad, S. Water pollution: Major issue in urban areas. *Int. J. Water Resour. Environ. Eng.* **2012**, *4*, 55–65.
16. Takada, K.; Nakamura, A.; Matsuo, N.; Inoue, A.; Someya, K.; Shimogaki, H. Influence of Oxidative and/or Reductive Treatment on Human Hair (I): Analysis of Hair-Damage after Oxidative and/or Reductive Treatment. *J. Oleo Sci.* **2003**, *52*, 541–548. [[CrossRef](#)]
17. Mistry, N. Guidelines for Formulating Anti-Pollution Products. *Cosmetics* **2017**, *4*, 57. [[CrossRef](#)]
18. Musilova, J.; Árvay, J.; Vollmannová, A.; Toth, T.; Tomas, J. Environmental Contamination by Heavy Metals in Region with Previous Mining Activity. *Bull. Environ. Contam. Toxicol.* **2016**, *97*, 569–575. [[CrossRef](#)] [[PubMed](#)]
19. Wolfsperger, M.; Hauser, G.; Gößler, W.; Schlagenhaufen, C. Heavy metals in human hair samples from Austria and Italy: Influence of sex and smoking habits. *Sci. Total Environ.* **1994**, *156*, 235–242. [[CrossRef](#)]
20. Srogi, K. Heavy metals in human hair samples from Silesia Province: The influence of sex, age and smoking habit. *Probl. Forensic Sci.* **2004**, *11*, 7–27.
21. Choon Teck, L. Human Hair Keratin and Its Interaction with Metal Ions. Master's Thesis, Nanyang Technology University, Singapore, 2020.
22. Sikorski, J.; Simpson, W.S. D.—'STUDIES OF THE REACTIVITY OF KERATIN WITH HEAVY METALS'. *J. R. Microsc. Soc.* **1958**, *78*, 35–39. [[CrossRef](#)]
23. Stadtman, E.R. Metal ion-catalyzed oxidation of proteins: Biochemical mechanism and biological consequences. *Free. Radic. Boil. Med.* **1990**, *9*, 315–325. [[CrossRef](#)]
24. Vergheese, P.S. Investigation of Toxic Heavy Metals in Drinking Water of Agra City, India. *Orient. J. Chem.* **2015**, *31*, 1835–1839. [[CrossRef](#)]
25. Gupta, P.; Diwan, B. Bacterial Exopolysaccharide mediated heavy metal removal: A Review on biosynthesis, mechanism and remediation strategies. *Biotechnol. Rep.* **2016**, *13*, 58–71. [[CrossRef](#)]
26. Goldstein, D.H. *Polarized Light. Revised and Expanded*; CRC Press: New York, NY, USA, 2003.
27. Desroches, J.; Pagnoux, D.; Louradour, F.; Barthélémy, A. Fiber-optic device for endoscopic polarization imaging. *Opt. Lett.* **2009**, *34*, 3409–3411. [[CrossRef](#)]
28. Lattouf, R.; Younes, R.; Lutomski, D.; Naaman, N.; Godeau, G.; Senni, K.; Changotade, S. Picrosirius Red Staining. *J. Histochem. Cytochem.* **2014**, *62*, 751–758. [[CrossRef](#)] [[PubMed](#)]
29. Peno-Mazzarino, L.; Desroches, J.; Percoco, G.; Faradova, U.; Laquerriere, K.; Scalvino, S.; Fays, C.; Judith, T.; Lati, E. The K-Probe@Imaging System as a New Tool to Analyze Human Skin Aging. Poster BIO-EC COMET 2019. Available online: http://www.kamax-innovative.com/download/Comet2019_BIOEC_KAMAX.pdf (accessed on 30 September 2020).
30. Yu, J.; Da-wen, Y.; Checkla, D.M.; Freedberg, I.M.; Bertolino, A.P. Human Hair Keratins. *J. Investig. Dermatol.* **1993**, *101*, 56S–59S. [[CrossRef](#)]

